

# Influence of Pore-Volume Topology of Zeolite ITQ-7 in Alkylation and Isomerization of Aromatic Compounds

A. Corma,<sup>\*,1</sup> V. I. Costa-Vaya,<sup>†</sup> M. J. Díaz-Cabañas,<sup>\*</sup> and F. J. Llopis<sup>†</sup>

<sup>\*</sup>Instituto de Tecnología Química, UPV-CSIC, Universidad Politécnica de Valencia, Avenida de los Naranjos s/n, 46022 Valencia, Spain; and <sup>†</sup>Departamento de Ingeniería Química, UVEG, Universitat de València, C/ Dr. Moliner, 50, 46100 Burjassot Valencia, Spain

Received September 25, 2001; revised December 12, 2001; accepted December 12, 2001

The void structure of zeolite ITQ-7 (ISV structure) is discussed on the basis of catalytic reaction tests. The isomerization and disproportionation of meta-xylene, and the alkylation of benzene or toluene with either ethanol or isopropanol, on the acidic zeolite have been used as model reactions. The dimensions of its three-dimensional system of channels, with pores between 6.1 and 6.3 Å and with lower tortuosity than those of beta zeolite, favor higher ratios of isomerization to disproportionation of meta-xylene, and of mono- to dialkylated products and iso- to *n*-propylbenzene during alkylation of benzene. These effects are enhanced with a partially coked ITQ-7. © 2002 Elsevier Science (USA)

**Key Words:** ITQ-7 zeolite; beta zeolite; meta-xylene isomerization; benzene alkylation; toluene alkylation; para-selectivity; cumene and ethylbenzene production on zeolites.

## INTRODUCTION

Zeolites are microporous solids that find a wide range of commercial applications in catalytic, adsorption, and separation processes (1–3). For some of these applications it is desirable to have a zeolite with a three-dimensional system of large pores, since this greatly facilitates the diffusion of relatively large molecules in and out of the zeolite void space, minimizing pore blockage. Additionally, it may also be important that the zeolite can be prepared with high Si/Al ratios, since this improves the chemical, thermal, and hydrothermal stability of the material. However, despite considerable synthetic efforts throughout the last decades, beta was the only known zeolite with a three-dimensional system of large pores that could be directly synthesized with Si/Al ratios higher than around 5 (4). Zeolite beta is a complex intergrown structure of at least two polymorphs, with large pores defined by 12-member-ring (MR) windows (5). Recently, three new three-dimensional 12-MR pore zeolites, ITQ-7, ITQ-16, and ITQ-17, have been synthesized. ITQ-17 (6, 7) corresponds to the pure polymorph C of beta, as was proposed by Newsam *et al.* (5), ITQ-16 (8) is formed

by the three polymorphs, A, B, and C, of beta, and ITQ-7 (9, 10) is structurally related to beta zeolite.

In the present work we have studied the catalytic behavior of Al-ITQ-7 (9) on alkylation and isomerization of aromatic compounds, and the results have been rationalized on the basis of the pore topology of this zeolite. It is shown that even if ITQ-7 is structurally related to beta zeolite, small differences in pore dimensions and pore architecture have a sensitive influence on product selectivity, making ITQ-7 appear to be an interesting catalyst for aromatic alkylation.

## EXPERIMENTAL

### Materials

Al-ITQ-7 (9) was prepared by first synthesizing a B-ITQ-7 which was subsequently exchanged following a method described previously (11). The B-ITQ-7 was synthesized using the hydroxide form of 1,3,3-trimethyl-6-azonium-tricyclo[3.2.1.4<sup>6,6</sup>] dodecane as structure-directing agent, and following the procedure described in (9). After 7 days of crystallization at 473 K in PTFE-lined stainless steel autoclaves at 60-rpm rotation, a powder was obtained that after calcination at 853 K yields a material whose XRD pattern corresponds to that of ITQ-7. The B-ITQ-7 was calcined at 853 K for 3 h and the resultant sample was exchanged with Al<sup>3+</sup>. This was repeatedly washed with H<sub>2</sub>O and the final material had a Si/Al ratio of 90, as determined by chemical analysis. A second ITQ-7 sample with a Si/Al ratio of 55 was prepared following the same procedure and exchanging twice with Al<sup>3+</sup>.

A beta zeolite sample with a Si/Al ratio of 50 was synthesized in fluoride medium from a gel with a molar composition: SiO<sub>2</sub> : 0.01 Al<sub>2</sub>O<sub>3</sub> : 0.55 TEAOH : 7.5 H<sub>2</sub>O : 0.55 HF. The preparation procedure was as follows: tetraethylorthosilicate (TEOS, Merck) was hydrolyzed under stirring in an aqueous solution of tetraethylammonium hydroxide (TEAOH, Aldrich). Then, a solution obtained by dissolving metallic aluminum in aqueous TEAOH was added and the mixture was kept under stirring until the ethanol formed and the hydrolysis of TEOS was evaporated. HF (48 wt %,

<sup>1</sup> To whom correspondence should be addressed. Fax: 34(96)3877809. E-mail: [acorma@itq.upv.es](mailto:acorma@itq.upv.es).

Aldrich) was added to the clear solution obtained, and a thick paste was formed. Finally, nanocrystalline zeolite beta was also added. The crystallization was carried out in Teflon-lined stainless steel autoclaves at 413 K under rotation (60 rpm) for 3 days. After this time, the solids were recovered by filtration and washed with distilled water. The acid zeolites were obtained by calcination at 853 K for 3 h. The samples were pelletized, crushed, and sieved, and the particles in the 0.3- to 0.5-mm range were used as catalysts.

Benzene, toluene, meta-xylene, ethanol, and 2-propanol were all analytical grade (Aldrich) reagents and were used without further purification. N<sub>2</sub> (99.999% purity) was used as carrier gas.

### Methods

X-ray powder diffraction (CuK $\alpha$  radiation) was used to determine the crystallinity of the solids. Measurements were recorded in a Philips X'Pert MPD diffractometer equipped with a PW3050 goniometer (CuK $\alpha$  radiation, graphite monochromator) provided with variable divergence and antiscatter slits and working in the fixed irradiated area mode. The chemical composition of the samples was obtained by chemical analysis using an atomic absorption spectrophotometer (Varian Spectra A-10 Plus) and results are given in Table 1.

Solid-state <sup>27</sup>Al NMR spectra were recorded under magic angle spinning (MAS) at room temperature in a Varian Unit VXR-400WB spectrometer at 104.2 MHz.

Acidity measurements were carried out by adsorption/desorption of pyridine followed by IR spectroscopy in a Nicolet 710 Fourier transform IR spectrophotometer equipped with Data Station. Self-supported wafers (10 mg cm<sup>-2</sup>) of calcined samples, previously activated at 673 K and 10<sup>-2</sup> Pa overnight in a Pyrex vacuum cell, were contacted with 6.5  $\times$  10<sup>-2</sup> Pa of pyridine vapor at room temperature

and desorbed in vacuum at increasing temperatures (423, 523, and 623 K). After each desorption step, the spectrum was recorded at room temperature and the background subtracted. Quantitative determination of the amount of Brønsted and Lewis acid sites was derived from the intensities of the IR bands at ca. 1450 and 1550 cm<sup>-1</sup>, respectively, using the extinction adsorption coefficients calculated by Emeis (12).

### Reaction Procedure

The catalytic reactions were conducted in vapor phase at atmospheric pressure in a fixed-bed continuous glass down-flow reactor (11-mm internal diameter). The catalyst was diluted with glass and located in the reactor bed, which was heated.

The meta-xylene isomerization was carried out with a meta-xylene/N<sub>2</sub> molar ratio of 0.25. In the alkylation reaction, benzene or toluene was fed in excess alcohol in a molar ratio of 4, while the N<sub>2</sub> flow was fixed to achieve a 1 : 10 molar ratio of N<sub>2</sub> to alcohol. Prior to addition of the reactants, the catalyst was heated to 623 K at a heating rate of 5 K/min, under a flow of nitrogen. After 30 min, the temperature was raised to 723 K and kept at that temperature for 1 h. The reactor was then cooled to reaction temperature: 623 K for meta-xylene isomerization, 573 K for toluene alkylation, or 553 K for benzene alkylation. When the temperature was stabilized, the reactants in liquid-phase were fed at the top of the reactor. The reactor exit was connected to a multisampling controlled heated valve equipped with a hydrocarbon detector at the outlet, in order to detect the moment when the products fill the first loop. This moment is considered the zero reaction time, and the gas sample is kept in the first loop. The rest of the loops were automatically filled at preprogrammed times on stream (10, 30, 60, 180, and 360 s). The products of the reactions were analyzed in a gas chromatograph (HP5890II) equipped with a Supelco-WAX10 capillary column (60-m length, 0.2-mm inner diameter) and a flame ionization detector.

Preliminary experiments were done in order to establish the conditions for which no control by external or internal diffusion exists. As the catalytic activity of the different zeolites differed substantially, the amount of catalyst in the reactor and the molar flow of reactants were adapted to obtain the desired degree of conversion. Initial selectivities were obtained from the initial rates of formation of the products. Initial rates were calculated from the initial conversions,  $X_0$ , by extrapolating the conversion  $X$ , measured at different times-on-stream ( $t$ ) according to the following equation:

$$X = X_0 \exp(-kt^{1/2}). \quad [1]$$

Initial rates were obtained by fitting conversion versus contact time to the equation

$$X_0 = r_0(W_{\text{cat}}/F_0). \quad [2]$$

TABLE 1

Characteristics of Samples Used in This Work

Sample	ITQ-7A	ITQ-7B	Beta
Si/Al ratio (chemical analysis)	90	55	50
Area BET (m <sup>2</sup> /g)	423	575	488
Crystal size ( $\mu$ m)	1–2	0.2–0.3	0.3–0.5
Brønsted acidity ( $\mu$ mol Py/g)			
$T = 423$ K	7	27	21
$T = 523$ K	6	21	20
$T = 623$ K	5	9	18
Lewis acidity ( $\mu$ mol Py/g)			
$T = 423$ K	8	20	16
$T = 523$ K	8	17	10
$T = 623$ K	7	17	8

*Note.* Crystal size estimated from SEM pictures. Acidity and acid strength distribution determined by IR-pyridine measurements at different desorption temperatures, using the extinction molar coefficients given by Emeis (12).

## RESULTS AND DISCUSSION

Two types of reactions have been carried out: meta-xylene isomerization and disproportionation, and benzene and toluene alkylation with ethanol and isopropanol. It is known (13, 14) that xylene isomerization–transalkylation requires strong acid sites and that benzene and toluene alkylation works with weak and medium acidity.

*Xylene Isomerization–Disproportionation*

The isomerization and disproportionation of meta-xylene has been proposed as a test reaction which allows differentiation between 10- and 12-MR pore zeolites, while indicating whether there are lobes, cages, or crossing channels (13–19). This is based on the fact that during isomerization of meta-xylene, both para- and ortho-xylenes are formed and, at low levels of conversion, 10-MR pore zeolites give higher para/ortho ratios (p/o) than 12-MR zeolites. This is owed to differences in the diffusion of both isomers through the narrower channels of the 10-MR zeolites (20), together with the larger transition state for ortho-xylene than for para-xylene formation (18). Moreover, the disproportionation of xylenes to give trimethylbenzenes and toluene is a bimolecular reaction, which involves a much bulkier reaction transition state than the monomolecular isomerization process. It is clear that the ratio of isomerization to disproportionation (i/d) will give an indication of the presence of lobes, cavities, or crossing channels where the available space will be large enough to allow the bimolecular reaction to occur.

Figure 1 shows the activity for meta-xylene isomerization and disproportionation with beta and ITQ-7 zeolites, with

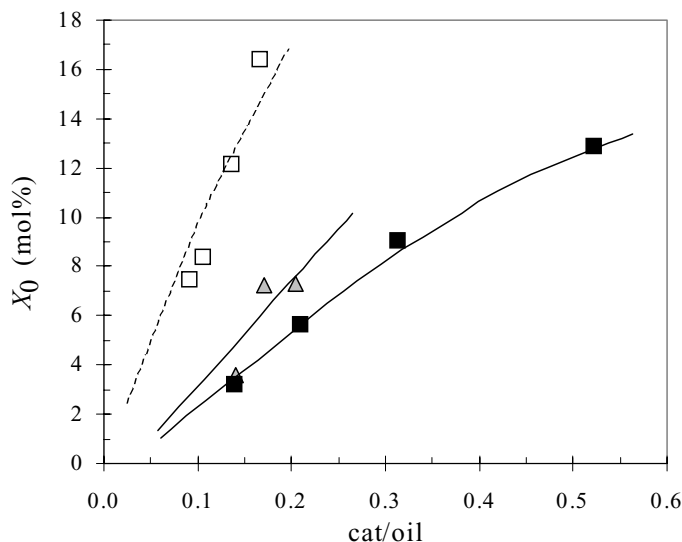


FIG. 1. Initial conversion in the isomerization and disproportionation of *m*-xylene at 623 K and 0.2 atm partial pressure, over zeolites ITQ-7A (■), ITQ-7B (Δ), and beta (□).

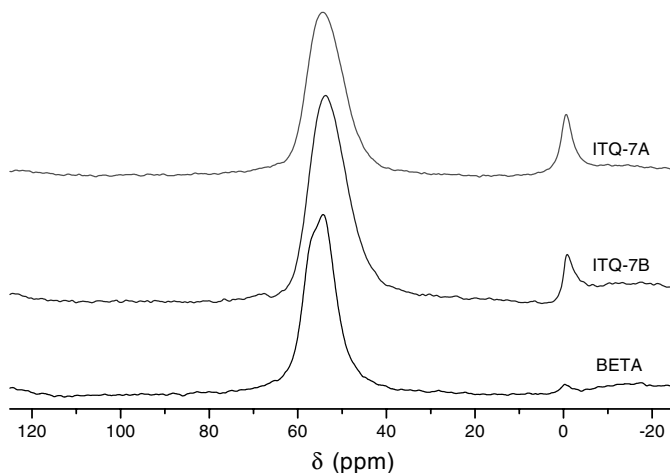


FIG. 2.  $^{27}\text{Al}$  MAS NMR spectra of ITQ-7A, ITQ-7B, and beta zeolites after calcination.

the activity of the former being higher than that of ITQ-7. However, this difference in activity can be explained on the basis of the difference in the framework of Si/Al and the number and strength of acid sites within the two zeolites (Table 1). Indeed, the number of the stronger Brønsted acid sites required to perform meta-xylene isomerization and disproportionation, which corresponds to those retaining pyridine at a 623 K desorption temperature, is larger in beta than in ITQ-7. Also  $^{27}\text{Al}$  MAS NMR results of ITQ-7 and beta show (Fig. 2) that a higher ratio of tetrahedrally to octahedrally coordinated aluminum,  $^{\text{IV}}\text{Al}/^{\text{VI}}\text{Al}$ , occurs in beta.

With respect to product selectivity, ITQ-7 and beta show a para/ortho value that is in the range expected for 12-MR zeolites (Table 2). However, when both zeolites are

TABLE 2

Para/Ortho Ratio, Isomerization/Disproportionation Ratio, and Distribution of Trimethylbenzenes at Low Conversions of *m*-Xylene on Different Zeolites

Zeolite	$X_0$ (mol %)	p/o	i/d	Trimethylbenzene (%)			1,2,3/1,3,5 ratio
				1,3,5	1,2,4	1,2,3	
ITQ-7A	3.2	0.94	3.1	14.0	79.7	6.3	0.45
	5.6	1.10	3.4	13.3	80.5	6.2	0.47
	12.8	1.29	4.8	22.5	69.3	8.2	0.37
ITQ-7B	3.6	0.88	4.0	13.3	80.5	6.2	0.47
	7.4	1.05	3.7	17.3	75.6	7.1	0.41
	7.6	1.16	3.8	21.7	70.6	7.7	0.36
Beta	7.5	1.21	2.5	23.8	69.0	7.2	0.30
	8.4	1.28	2.9	24.4	68.6	7.0	0.29
	12.1	1.30	2.8	24.2	68.1	7.7	0.32
	Equilibrium (623 K)	1.0		24.0	68.0	8.0	0.33

<sup>a</sup> Ref. (15).

compared in i/d ratio, small but significant differences exist. At the same level of total conversion ITQ-7 always gives a higher i/d ratio. Then, smaller void volumes in the structure can be expected in ITQ-7 samples.

An additional selectivity parameter, which can be highly informative for the presence of internal cages, lobes, or channel crossing, is the distribution of the trimethylbenzene (TMB) products formed by disproportionation of meta-xylene. Indeed, this reaction occurs through the formation of three possible 1,1-diphenylmethane-type transition states (21–24), leading to the 1,2,4-, 1,3,5-, and 1,2,3-TMB isomers. None of the three transition state complexes can be easily accommodated in the pores of the 10-MR zeolites, and when small amounts of disproportionation occur, the less impeded complex, which leads to the formation of 1,2,4-TMB, should be favored. In Table 2, the distribution of the trimethylbenzenes obtained with zeolite ITQ-7, at low levels of meta-xylene conversion, is compared with that obtained with ZSM-5 and beta zeolites. It can be seen there that 1,2,4-TMB is initially formed on ITQ-7 in amounts larger than on beta zeolite and above the thermodynamic equilibrium, while 1,3,5- and 1,2,3-TMB were formed in lower amounts than those predicted by the thermodynamic equilibrium. The analysis of these results indicates that the less bulky bimolecular transition state (1,2,4-TMB) is clearly favored in the case of ITQ-7 with respect to beta zeolite. This should be due to the presence of smaller void volumes and/or to the presence of smaller and less sinusoidal pores in ITQ-7 than in beta zeolite.

The ratio of the initial selectivities for 1,2,3- to 1,3,5-TMB obtained at low levels of disproportionation seems to reflect the shape of the pores. In lobate pores (FAU or L zeolites) the ratio is lower than in zeolites in which the configuration of the side pockets and side channels does not create regular lobes (OFF, MOR, Omega) (18). In a straight pore with side pockets at regular distances the ratio of 1,2,3-/1,3,5-TMB is initially high, while for 12-MR zeolites consisting of alternating cages or lobes separated by a 12-MR, this ratio is much lower. The ratio of those trimethylbenzene isomers for the zeolite ITQ-7, shown in Table 2, is higher than that for the beta zeolite, indicating that the reactants see smaller void spaces in the ITQ-7 than in beta. It should be taken into account that the results are not masked by the reaction at the external surface since the crystallite size of ITQ-7B and beta is very similar (Table 1).

### Benzene and Toluene Alkylation

The alkylation of benzene or toluene with alkenes or alcohols are reactions of commercial interest that produce alkylaromatics such as ethylbenzene, xylenes, cumene, ethyltoluenes, cymenes, etc. (25–27). The catalytic synthesis in superacid media of alkylaromatics from alkenes or alcohols was reported by Schmerling and Vesely (28) and Olah *et al.* (29). These catalysts showed high catalytic activity and

selectivity. However, they present environmental problems and corrosion. These drawbacks can be overcome by using solid catalysts. In view of this, over the past few years, important efforts have been made to develop heterogeneous systems for this process. In particular, zeolite-type solid acids were reported to produce alkylbenzenes from aromatics and light olefins or alcohols (30–34), and the reaction pathway leading to alkylaromatics in the presence of zeolites was found to be much more complex than in the case of conventional acids (35, 36).

The alkylation of benzene or toluene with ethanol or propanol can be considered an electrophilic substitution on the aromatic ring. Alkylation reactions catalyzed by acidic zeolites are commonly considered as proceeding via a carbenium ion-type mechanism (32). When alcohol is used as an alkylating agent, the isopropylation or ethylation reaction is proposed to take place by the reaction of the

TABLE 3  
Conversion and Product Distribution in Benzene Alkylation with Ethanol and Isopropanol over ITQ-7 and Beta Samples

Sample	Ethanol			Isopropanol		
	ITQ-7A	ITQ-7B	Beta	ITQ-7A	ITQ-7B	Beta
Weight catalysts (mg)	51.2	57.2	43.8	51.2	40.1	43.8
WHSV (min <sup>-1</sup> )	3.4	6.0	4.7	3.4	7.5	6.9
Benzene conversion (mol%) <sup>a</sup>	3.7	3.6	5.0	9.5	11.7	10.1
Alcohol conversion (mol%) <sup>a</sup>	31.2	40.5	47.7	98.5	98.5	96.1
Alcohol yield in products (%)						
Olefins & oligomers	18.5	25.1	25.6	69.1	63.5	62.9
Aromatics	12.7	15.4	22.1	29.4	35.0	33.2
No reaction	68.8	59.5	52.3	1.5	1.5	3.9
Aromatic product distribution (%) <sup>b</sup>						
Toluene	3.9	0.9	0.2	1.0	0.8	1.3
Ethylbenzene	84.0	83.8	76.2	1.1	1.5	0.5
Xylenes	0.0	0.0	1.9	0.0	0.0	0.0
Cumene	0.0	0.0	0.4	80.6	81.2	81.3
<i>n</i> -Propylbenzene	0.0	0.0	0.0	0.4	0.6	0.7
Butylbenzenes	0.0	0.0	0.0	0.4	0.5	0.4
Diethylbenzenes	9.4	10.8	11.5	—	—	—
Diisopropylbenzenes	—	—	—	16.3	15.4	15.8
Triethylbenzenes	2.7	4.5	8.2	—	—	—
Others aromatics	0.0	0.0	1.5	0.1	0.1	1.0
Normalized distributions (%) <sup>c</sup>						
Diethylbenzenes						
Para	24.2	24.5	20.3	31.7	32.4	33.9
Meta	34.8	37.8	46.1	67.2	67.	64.2
Ortho	41.0	37.8	33.6	1.1	0.5	1.9
Diisopropylbenzenes						

Note. Reaction conditions: benzene-to-ethanol molar ratio, 4; benzene-to-isopropanol molar ratio, 4; temperature, 553 K.

<sup>a</sup> Benzene and alcohol conversions obtained at 30 s time-on-stream.

<sup>b</sup> Benzene free.

<sup>c</sup> Calculated thermodynamic equilibria at 553 K give a para/meta/ortho distribution of diethylbenzenes of 32/56.5/11.5 and of diisopropylbenzenes of 32/58.1/9.9.

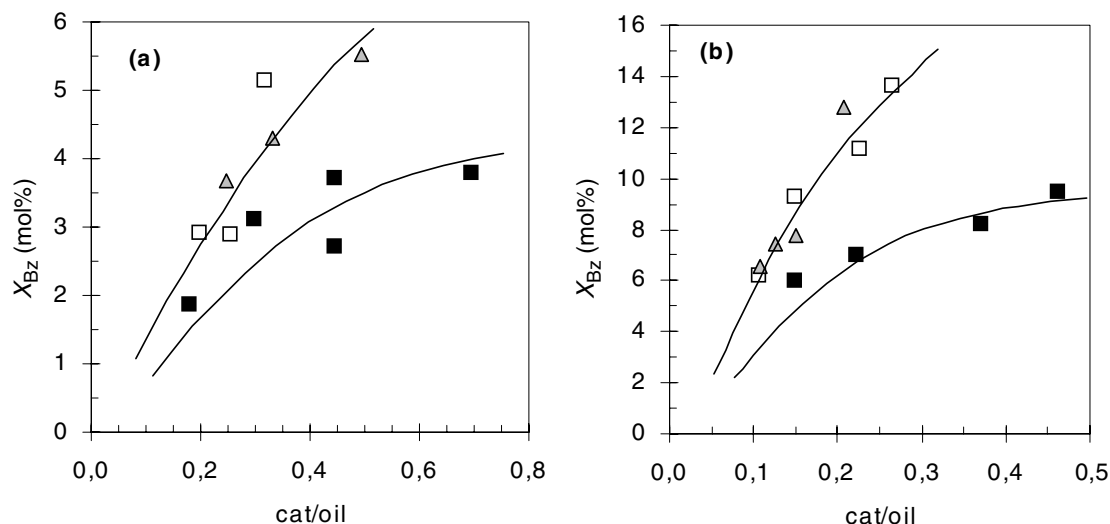


FIG. 3. Benzene conversion in the alkylation process at 553 K and 30 s time-on-stream, for a benzene-to-alcohol molar ratio in feed of 4, over zeolites ITQ-7A (■), ITQ-7B (Δ), and beta (□) versus cat/oil (g · h/mol). (a) Benzene alkylation with ethanol and (b) benzene alkylation with isopropanol.

activated alkene (formed by dehydration of the alcohol) on the acid sites of the zeolite. When the olefin is activated on the Brønsted acid site, it can react with benzene or toluene, producing monoalkylated or polyalkylated aromatics, or with another propanol or ethanol molecule, producing C6, C8, or C9 species; which can be further transformed through oligomerization, cracking, isomerization and alkylation reactions, producing olefins (mainly ethylene and propylene oligomers), paraffins, and other alkylbenzenes (butylbenzenes, pentylbenzenes, etc.).

Tables 3 and 4 present conversion and selectivity results for the alkylation of benzene and toluene with ethanol and propanol over ITQ-7 and beta zeolites. It is seen that the main product for benzene ethylation (Table 3) is ethylbenzene, followed by diethylbenzenes and triethylbenzenes. Toluene and other aromatics appear in much lower amounts. Meanwhile, in the propylation of benzene the main product is cumene, together with diisopropylbenzenes. Toluene, ethylbenzene, and butylbenzenes are obtained in low concentrations. *n*-Propylbenzene is also produced via secondary transalkylation of cumene with benzene (37), and it should be noted that in an industrial process, the presence of *n*-propylbenzene affects negatively both the yield and the quality of the product (38). Figures 3a and 3b show benzene conversion in alkylation with ethanol and isopropanol, respectively.

In the case of toluene ethylation (Table 4), the main products are ethyltoluenes, followed by diethyltoluenes and other alkylaromatics of high molecular weight. In addition, benzene, ethylbenzene, and xylenes can be obtained in substantially lower amounts, especially in ITQ-7. Finally, the main products in the propylation of toluene are cymenes (isopropyltoluenes), together with benzene, cumene, xylenes, and other alkylaromatics in low concentrations.

TABLE 4

Conversion and Product distribution in Toluene Alkylation with Ethanol and Isopropanol over ITQ-7 and Beta Samples

Sample	Ethanol			Isopropanol		
	ITQ-7A	ITQ-7B	Beta	ITQ-7A	ITQ-7B	Beta
Weight catalysts (mg)	42.8	18.4	43.8	42.8	18.4	43.8
WHSV (min <sup>-1</sup> )	5.0	9.3	4.9	7.0	9.3	7.8
Toluene conversion (mol%) <sup>a</sup>	10.8	6.7	14.8	11.4	10.7	11.0
Alcohol conversion (mol%) <sup>a</sup>	14.4	21.2	16.2	90.8	87.6	97.6
Alcohol yield in products (%)						
Olefins & oligomers	5.2	11.6	7.1	66.5	54.8	64.6
Aromatics	9.3	9.6	9.0	24.3	32.8	33.0
No reaction	85.5	78.8	83.9	9.2	12.4	2.4
Aromatic product distribution (%) <sup>b</sup>						
Benzene	0.3	0.0	0.2	0.5	0.7	0.7
Ethylbenzene	0.0	0.9	0.1	0.0	0.0	0.0
Xylenes	0.7	0.0	0.6	0.5	1.4	1.2
Cumene	0.0	0.0	0.0	1.1	1.7	1.6
Ethyltoluenes	69.8	72.1	58.5	—	—	—
Cymenes	—	—	—	94.4	94.1	92.6
Propyltoluenes	—	—	—	0.3	0.5	0.6
Diethyltoluenes	12.6	15.6	17.1	—	—	—
Others aromatics	16.6	10.5	23.5	3.2	1.7	3.3
Normalized distributions (%) <sup>c</sup>						
	Ethyltoluenes			Cymenes		
Para	25.6	26.0	24.7	33.1	29.7	34.8
Meta	29.2	28.5	32.2	55.5	60.9	54.5
Ortho	45.2	45.5	43.1	11.4	9.4	10.6

Note. Reaction conditions: toluene-to-ethanol molar ratio, 4; toluene-to-isopropanol molar ratio, 4; temperature, 573 K.

<sup>a</sup> Toluene and alcohol conversions obtained at 30 s time-on-stream.

<sup>b</sup> Toluene free.

<sup>c</sup> Calculated thermodynamic equilibria at 573 K give a para/meta/ortho distribution of ethyltoluenes of 34.1/50.0/15.9 and of cymenes of 22.6/63.2/14.2.

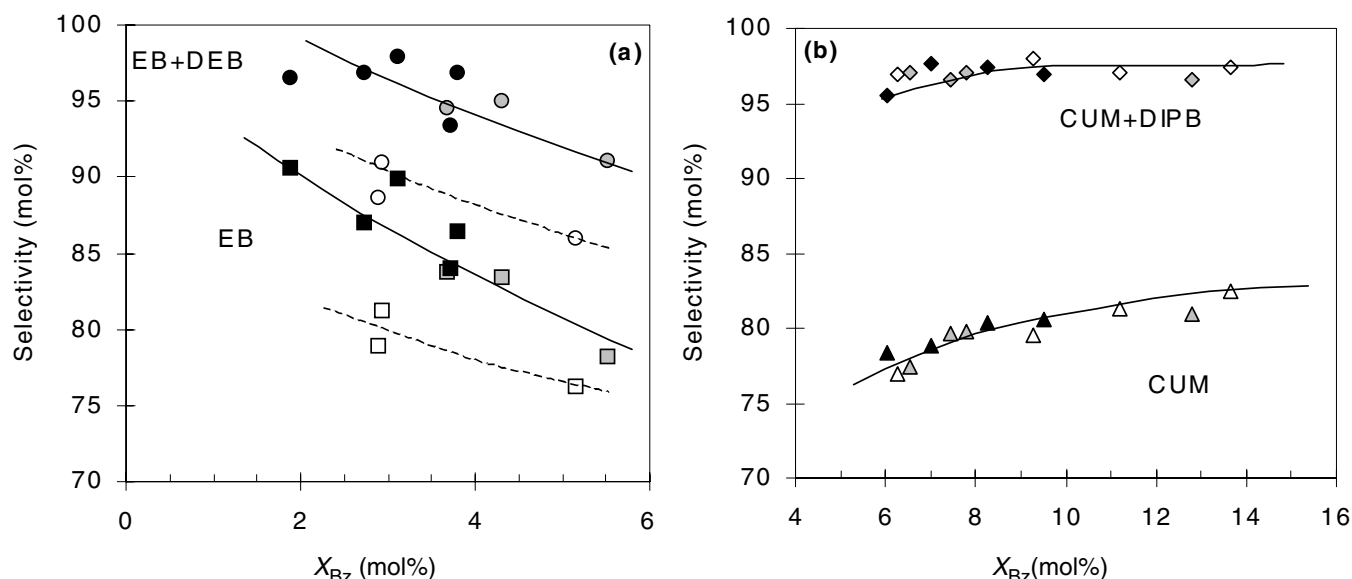


FIG. 4. Aromatic selectivity of zeolites ITQ-7A (filled dot), ITQ-7B (grey dot), and beta (open dot) as follows. (a) In benzene alkylation with ethanol: ethylbenzene (EB, ■, □, ◻); ethyl plus diethylbenzenes (EB + DEB, ●, ○, ◐). (b) In benzene alkylation with isopropanol: cumene (CUM, ▲, △, △); cumene plus diisopropylbenzenes (CUM + DIPB, ◆, ◇, ◇).

*n*-Propyltoluenes are also produced via secondary trans-alkylation of cymenes with toluene (37).

It is surprising that aromatic selectivity to ethyltoluenes obtained in toluene alkylation with ethanol is much higher with ITQ-7 than with beta (Table 4). In an analogous way, the aromatic selectivity to ethylbenzene in benzene alkylation with ethanol and the sum of selectivities to ethylbenzene and the corresponding dialkylated products are larger with ITQ-7 than with beta zeolite (Table 3). This is observed regardless of the level of conversion at which selectivities are compared (Figs. 4a and 5a). On the

other hand, cymenes prevail among the products obtained during the alkylation of toluene with isopropanol, giving values higher than 90% in the selectivity of aromatics for ITQ-7 and beta zeolites. Similarly, cumene is the main product in alkylation of benzene, with isopropanol again being the selectivity very similar for the two zeolites, regardless of conversion level (Figs. 4b and 5b).

The selectivity differences observed for ethylbenzenes, ethyltoluenes, diethylbenzenes, and diethyltoluenes produced on ITQ-7 and beta can be related to the channel structure of the two zeolites and to differences in the kinetic

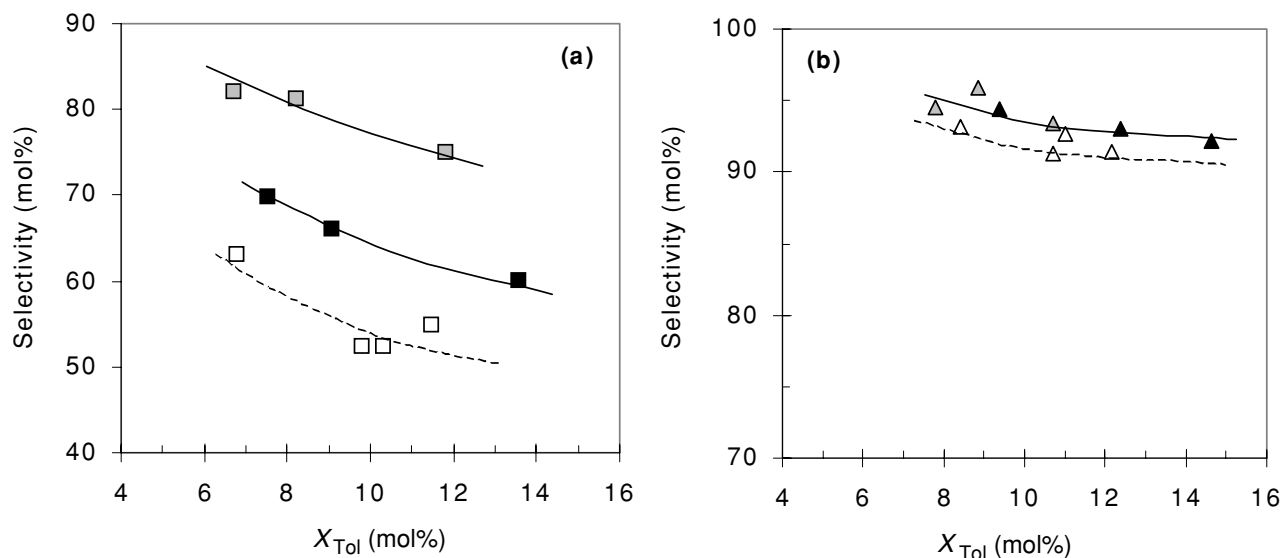


FIG. 5. Aromatic selectivity of zeolites ITQ-7A (filled dot), ITQ-7B (grey dot), and beta (open dot) as follows. (a) In toluene alkylation with ethanol: ethyltoluene (ET, ■, □, ◻). (b) In toluene alkylation with isopropanol: cymene (CYM, ▲, △, △).

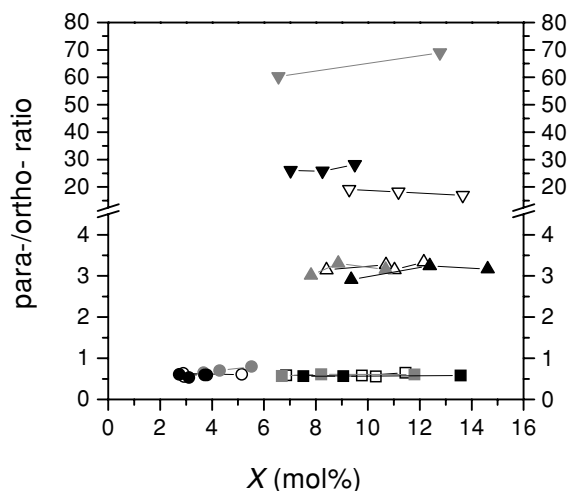


FIG. 6. Para/ortho ratio behavior of ITQ-7A (filled dot), ITQ-7B (grey dot), and beta (open dot) zeolites for benzene and toluene alkylation with ethanol and isopropanol: p/o-DEB (●, ○), p/o-ET (■, □), p/o-CYM (▲, △), p/o-DIPB (▼, ▽).

diameter of the aromatic molecules produced. In this way, the selectivity to monoalkylated products, i.e., ethylbenzene and ethyltoluene, is larger with ITQ-7 than with beta due to the more important pore restrictions existing in the former for formation and diffusion of the dialkylated and trialkylated products. Meanwhile, in alkylation of benzene or toluene with isopropanol, the different size increments of the alkylaromatics formed do not cause differences in diffusion of cumene and cymene within the two zeolite structures studied here. According to Hurgobin *et al.* (39), selectivity to cumene and diisopropylbenzenes or cymenes increased as conversion of propanol decreased, due to loss in activ-

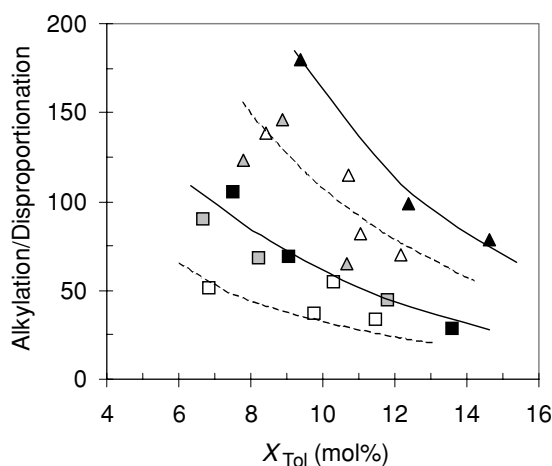


FIG. 7. Alkylation/disproportionation ratio of zeolites ITQ-7A (filled dot), ITQ-7B (grey dot), and beta (open dot) in toluene alkylation with ethanol and isopropanol: ethyltoluenes/xylenes (■, □), cymenes/xylenes (▲, △).

ity of the sites favoring propanol oligomerization. Then, a significant amount of the reaction may take place on the external surface of the zeolites due to pore blockage by coke.

#### Para-Selectivity

Figure 6 depicts the para/ortho ratio (p/o) of the iso-mers produced in aromatic alkylation reactions. If one takes into account the fact that the molecular size of those increases in the order ethyltoluene, diethylbenzene, cymene, diisopropylbenzene, we can predict that the experimental para-to-ortho ratio should increase when increasing the

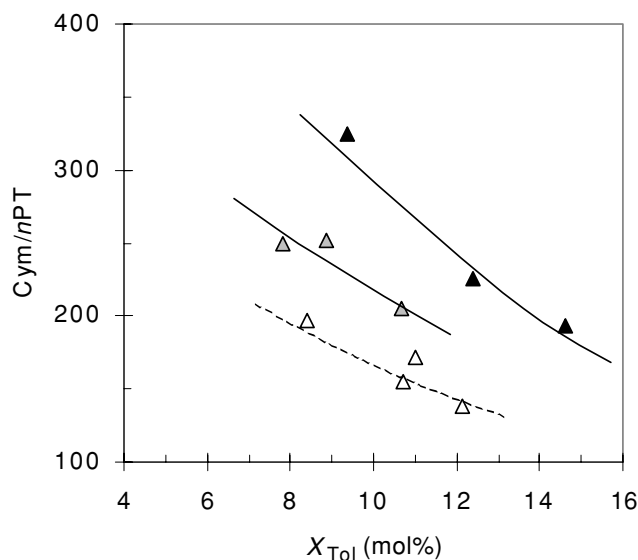
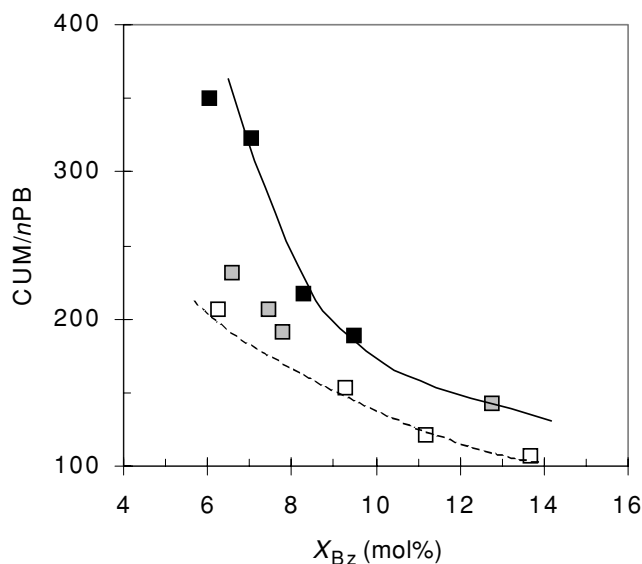


FIG. 8. Iso-/n-propylaromatic ratio of ITQ-7A (filled dot), ITQ-7B (grey dot), and beta (open dot) zeolites for benzene and toluene alkylation with isopropanol: cumene/n-propylbenzene (■, □); cymenes/n-propyltoluenes (▲, △).

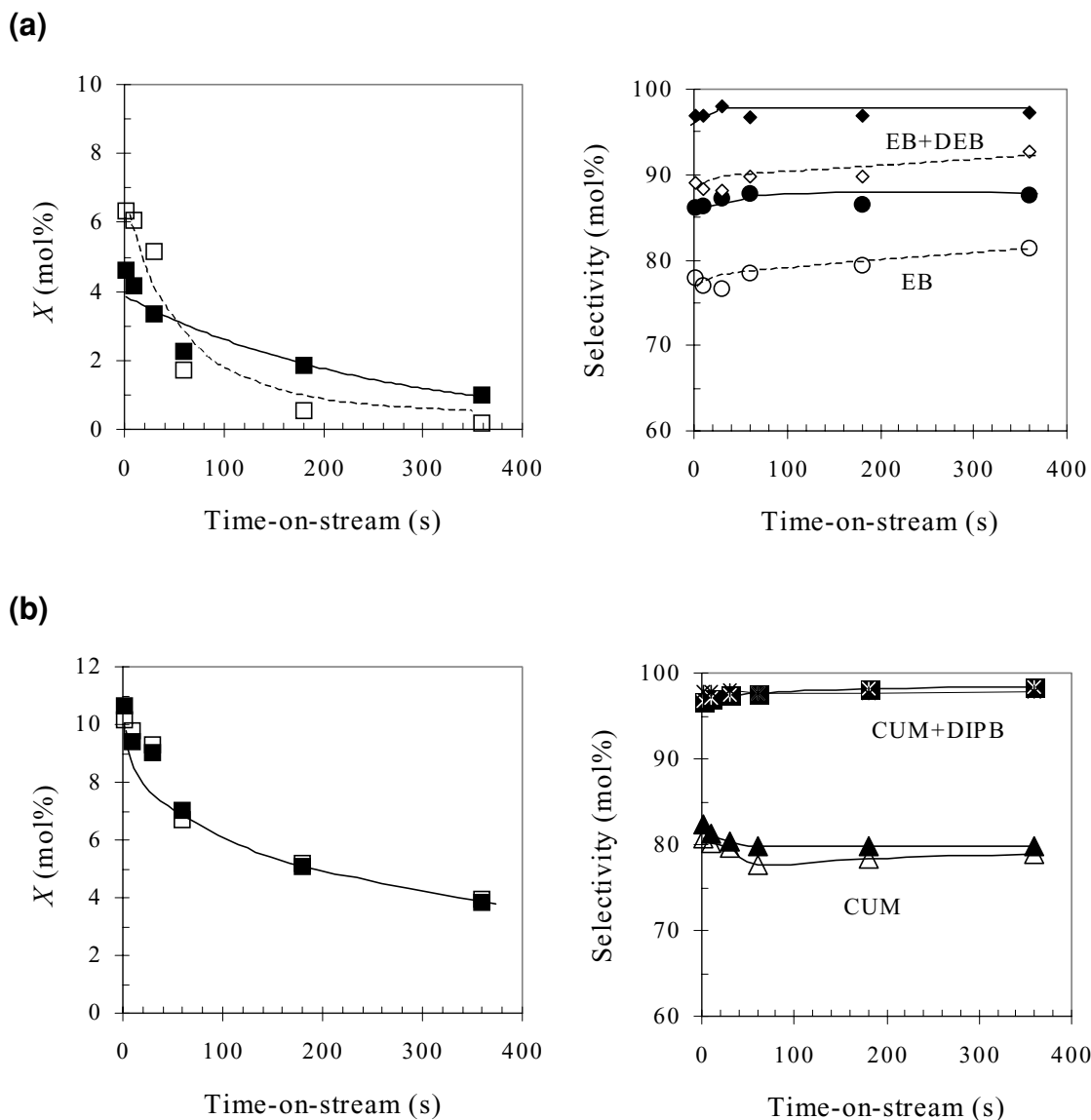


FIG. 9. Time-on-stream behavior of ITQ-7A (filled dot) and beta (open dot) zeolites for benzene alkylation with ethanol (a) and isopropanol (b). Conversion (■, □). Aromatic selectivity: ethylbenzene (EB, ●, ○), ethylbenzene plus diethylbenzenes (EB + DEB, ◆, ◇), cumene (CUM, ▲, △), cumene plus diisopropylbenzenes (CUM + DIPB, ■, \*).

molecular size of the products ( $p/o\text{-ET} < p/o\text{-DEB} < p/o\text{-Cym} < p/o\text{-DIPB}$ ). This indeed occurs for  $p/o$ -cymene and  $p/o$ -diisopropylbenzene, for which a higher para-to-ortho ratio is obtained with ITQ-7 zeolite.

As could be expected, zeolite crystal size can play an important role in the para-to-ortho ratio obtained, as shown in Fig. 6 for different crystal sizes of ITQ-7 samples. In any case, it appears that the diffusion of ortho-diisopropylbenzene is relatively slower in ITQ-7 than in beta zeolite, showing again that subtle differences in pore dimensions and topology can significantly affect selectivity, even in the case of 12-MR zeolites.

### Toluene Disproportionation

Toluene disproportionation is a commercial process for the production of benzene and xylenes, which are catalyzed by acid zeolites (41–43). The use of ZSM-5 zeolite as catalyst is especially interesting due to its high resistance to deactivation by coking and to the possibility of directing the reaction toward the formation of the most valuable para-xylene isomer when the zeolite is modified with different agents (17, 43–45). Disproportionation of toluene over zeolite beta has also been reported (46, 47), and interesting results have been obtained owing to its excellent stability.



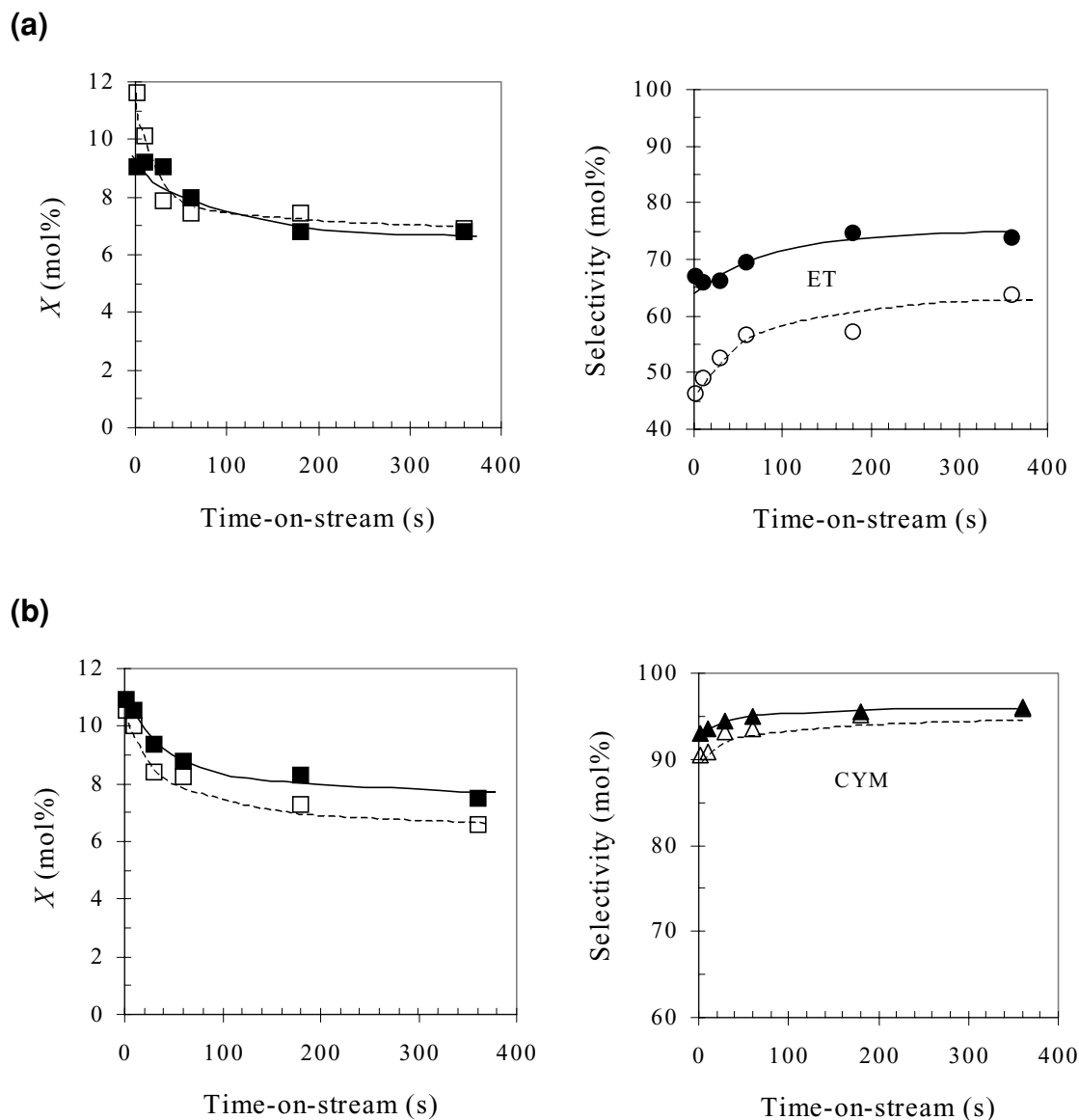


FIG. 10. Time-on-stream behavior of ITQ-7A (filled dot) and beta (open dot) zeolites ITQ-7A and beta zeolites for toluene alkylation with (a) ethanol and (b) isopropanol. Conversion (■, □). Aromatic selectivity: ethyltoluenes (ET, ●, ○), cymenes (CYM, ▲, △).

While beta zeolite cannot compete with ZSM-5 for disproportionation of toluene, it can be of practical interest for disproportionation–dealkylation of bulkier alkylaromatics (48).

When comparing ITQ-7 and beta zeolites, it is clear that disproportionation occurs to a lesser extent with ITQ-7 than with beta, and the difference increases when increasing the size of the alkylaromatics (Fig. 7).

#### *Iso- and *n*-Propyl Alkylaromatics*

In spite of the fact that there are numerous studies in the literature on the propylation of benzene or toluene over large- and medium-pore zeolites, the mechanism of

formation of *n*-propyl aromatics, the main undesired product, has not been elucidated until recently (49, 50). Initially, *n*-propyl aromatics were supposed to be generated via monomolecular isomerization of the isopropyl isomers formed in the first alkylation step (26). However, it has now been shown (50–52) that the formation of *n*-propyl isomers is the result of a transalkylation reaction of cumene with benzene or cymene with toluene. Ivanova and Fajula (35), studying the alkylation of benzene with labeled propylene on HZSM-11 by *in situ*  $^{13}\text{C}$  MAS NMR, came to the conclusion that *n*-propylbenzene formation takes place via an intermolecular reaction between cumene and benzene. When only isopropylbenzene or isopropyltoluenes were contacted with the zeolites, no *n*-propyl isomers were

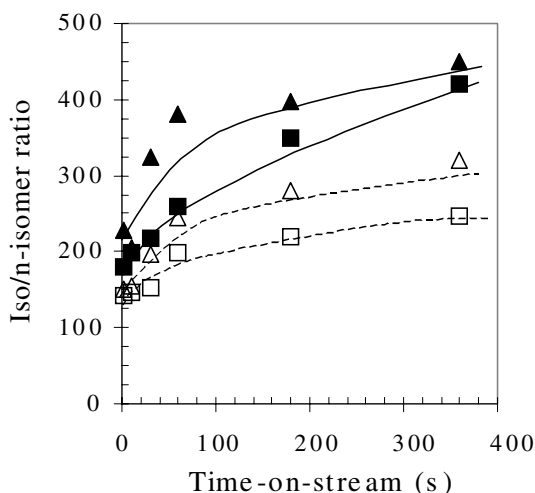


FIG. 11. Time-on-stream behavior of ITQ-7A (filled dot) and beta (open dot) zeolites in the iso-*n*-propylaromatic ratio of benzene and toluene process with isopropanol:cumene/*n*-propylbenzene (■, □); cymenes/*n*-propyltoluenes (▲, △).

detected. Wichterlová and Cejka (49) have found that the formation of *n*-propyltoluenes is strongly dependent on dimensions and architecture of the channels of the molecular sieve.

In the case of ITQ-7 and beta zeolites, the former produces, especially at low conversions, higher ratios of cumene to *n*-propylbenzene and cymenes to *n*-propyltoluenes (Fig. 8). This difference seems more significant in ITQ-7A samples, where Si/Al ratios and crystal sizes are larger. This would be in agreement with the lower selectivity of ITQ-7 than beta for disproportionation reactions, owing to the smaller size of the internal void volume.

### Catalyst Deactivation

We analyzed the influence of the reaction time-on-stream (TOS) on catalyst behavior, and the evolution of conversion and selectivity to the main products, in each alkylation process, versus TOS are presented in Figs. 9 and 10.

It can be seen that, for benzene ethylation, conversion decreases with time-on-stream regardless of the catalyst used. Nevertheless, this deactivation is larger for beta than for ITQ-7 zeolite (Fig. 9a). With respect to selectivity, only a slight increment of selectivity to ethylbenzene is observed when increasing TOS, but, nevertheless, the fact that the level of conversion decreases when increasing TOS should be considered. A decrease in conversion with TOS is also observed in benzene alkylation with isopropanol (Fig. 9b). A slight decrease in selectivity to cumene is accompanied by a slight increase in diisopropylbenzenes when increasing TOS, the behavior being very similar for both zeolites. This is probably a consequence of pore blocking, with the external surface having a higher impact on product distribution.

In the case of toluene alkylation with ethanol or isopropanol, a more significant decrease in conversion when increasing TOS can be seen for the beta sample (Fig. 10), together with an increase in selectivity to the main alkylation product. Note that coke deposition not only reduces the void space inside the channels, it also poisons active sites, diminishing their density. These two effects can explain the observed increase in the ratio of iso- to *n*-propyl when increasing TOS. This increase is larger for ITQ-7 (Fig. 11), whose behavior comes closer to that of the ZSM-5 zeolite with respect to iso/*n*-propylbenzene and toluene, at longer time-on-stream when the catalyst is partially coked.

### CONCLUSIONS

Al-ITQ-7 is an active zeolite for isomerization, disproportionation, and alkylation of alkylaromatics. Even if the structure of ITQ-7 and beta are related, the differences in pore dimensions and topology between the two zeolites have a clear impact on product selectivity. The differences are specially noticeable for alkylation of benzene and toluene with ethanol and isopropanol. For those reactions, ITQ-7 gives higher ratios of mono- to dialkylated products and iso- to *n*-propylbenzene or toluene than does beta zeolite. This behavior is enhanced with partially coked zeolites. This way, ITQ-7 appears to be an interesting catalyst for producing cumene and cymenes by alkylation of aromatics using alcohols or olefins, the low amount of *n*-propylbenzene formed being of special interest.

### ACKNOWLEDGMENTS

V. Costa-Vayá thanks the Conselleria de Cultura, Educación y Ciencia de la Generalitat Valenciana for scholarships. The authors thank the CICYT (MAT2000-1392) for financial support.

### REFERENCES

- Kühl, G. H., and Kresge, C. T., *Kirk Othmer 4th Encycl. Chem. Technol.* **16**, 888 (1995).
- Rabo, J. A., in "Guidelines to the Mastering of Zeolite Properties" (D. Barthomeuf, Ed.), p. 68. Plenum, New York, 1990.
- Chen, N. Y., Garwood, W. E., and Dwyer, F. G., "Shape-Selective Catalysis in Industrial Applications." Dekker, New York, 1989.
- Wadlinger, R. L., Kerr, G. T., and Rosinski, E. J., U.S. Patent A3,308,069 (1967).
- Newsam, J. M., Treacy, M. M., Jr., Koetsier, W. T., and Gruyter, C. B., *Proc. R. Soc. London Ser. A* **420**, 375 (1988).
- Corma, A., Navarro, M. T., Rey, F., Rius, J., and Valencia, S., *Angew. Chem. Int. Ed. Engl.* **40**, 2277 (2001).
- Corma, A., Navarro, M. T., Rey, F., and Valencia, S., *Chem. Commun.* 1486 (2001).
- Corma, A., Navarro, M. T., Rey, F., and Valencia, S., *Chem. Commun.* 1720 (2001).
- Villaescusa, L. A., Barrett, Ph. A., and Cambor, M. A., *Angew. Chem. Int. Ed. Engl.* **38**, 1997 (1999).
- Corma, A., Díaz-Cabañas, M. J., and Fornés, V., *Angew. Chem. Int. Ed. Engl.* **39**, 2346 (2000).
- Lobo, R. F., and Davis, M. E., *Microporous Mater.* **3**, 61 (1994).

12. Emeis, C. A., *J. Catal.* **141**, 347 (1993).
13. Perez-Pariente, J., Sastre, E., Fornes, V., Martens, J. A., Jacobs, P. A., and Corma, A., *Appl. Catal.* **69**, 125 (1991).
14. Guisnet, M., Gnep, N. S., and Morin, S., *Microporous Mesoporous Mater.* **35–36**, 47 (2000).
15. Jacobs, P. A., and Martens, J. A., *Stud. Surf. Sci. Catal.* **28**, 23 (1986).
16. Young, L. B., Butter, S. A., and Kaeding, W. W., *J. Catal.* **76**, 418 (1982).
17. Olson, D. H., and Haag, W. O., *ACS Symp. Ser.* **248**, 275 (1984).
18. Martens, J. A., Pérez-Pariente, J., Sastre, E., Corma, A., and Jacobs, P. A., *Appl. Catal.* **45**, 85 (1988).
19. Corma, A., Corell, C., Llopis, F. J., Martinez, A., and Perez-Pariente, J., *Appl. Catal. A* **115**, 121 (1994).
20. Corma, A., *Microporous Mesoporous Mater.* **21**, 487 (1998).
21. Corma, A., Llopis, F. J., and Montón, J. B., *J. Catal.* **140**, 384 (1993).
22. Xiong, Y., Rodewald, P. G., and Chang, C. D., *J. Am. Chem. Soc.* **117**, 9427 (1995).
23. Santilli, D. S., *J. Catal.* **99**, 327 (1986).
24. Adair, B., Chen, C. Y., Wan, K. T., and Davis, M. E., *Microporous Mesoporous Mater.* **7**, 261 (1996).
25. Kaeding, W. W., Chu, C., Young, L. B., Weinstein, B., and Butter, S. A., *J. Catal.* **67**, 159 (1981).
26. Fraenkel, D., and Levy, M., *J. Catal.* **118**, 10 (1989).
27. Mirth, G., and Lercher, J. A., *J. Catal.* **147**, 199 (1994).
28. Schmerling, L., and Vesely, J. A., *J. Org. Chem.* **38**, 312 (1973).
29. Olah, G. A., Schilling, P., Starol, J. S., Halpern, Yu., and Olah, J. A., *J. Am. Chem. Soc.* **97**, 6807 (1975).
30. Halgeri, A. B., and Das, J., *Appl. Catal. A* **181**, 347 (1999).
31. Bellusi, G., Pazzucini, G., Perego, C., Girotti, G., and Terzoni, G., *J. Catal.* **157**, 227 (1995).
32. Siffert, S., Gaillard, L., and Su, B. L., *J. Mol. Catal. A* **153**, 267 (2000).
33. Perego, C., Amarilli, S., Millini, R., Bellussi, G., Girotti, G., and Terzoni, G., *Microporous Mater.* **6**, 395 (1996).
34. Corma, A., Martínez-Soria, V., and Schnoefeld, E., *J. Catal.* **192**, 163 (2000).
35. Ivanova, I. I., and Fajula, F., *Int. Zeolite Conf.* **12**, 2273 (1998).
36. Kato, S., Nakagawa, K., Ikenaga, N., and Suzuki, T., *Chem. Lett.* **3**, 207 (1999).
37. Wichterlová, B., Cejka, J., and Zilková, N., *Microporous Mater.* **6**, 405 (1996).
38. Cejka, J., Wichterlová, B., and Bednárová, S., *Appl. Catal. A* **79**, 215 (1991).
39. Hurgobin, S., Petrik, L. F., Jansen, J. C., and O'Connor, C. T., *Int. Zeolite Conf.* **12**, 1073 (1998).
40. Chen, N. Y., Degnan, T. F., Jr., and Smith, C. M., "Molecular Transport and Reaction in Zeolites: Design and Application of Shape Selective Catalysts." VCH, Weinheim/New York, 1994.
41. Haag, W. O., Olson, D. H., and Rodewald, P. G., U.S. Patent 4,358,395 (1982).
42. Beck, J. S., Olson, D. H., and McCullen, S. B., U.S. Patent 5,367,099 (1994).
43. Kaeding, W. W., Chu, C., Young, L. B., and Butter, S. A., *J. Catal.* **69**, 392 (1981).
44. Meshram, N. R., Hegde, S. G., Kulkarni, S. B., and Ratnasamy, P., *Appl. Catal. A* **8**, 359 (1983).
45. Uguina, M. A., Sotelo, J. L., Serrano, D. P., and Valverde, J. L., *Ind. Eng. Chem. Res.* **33**, 26 (1994).
46. Wang, I., Tsai, T. Ch., and Huang, Sh. T., *Ind. Eng. Chem. Res.* **29**, 2005 (1990).
47. Das, J., Bhat, Y. S., and Halgeri, A. B., *Catal. Lett.* **23**, 161 (1994).
48. Bandyopadhyay, R., Sugi, Y., Kubota, Y., and Rao, B. S., *Catal. Today* **44**, 245 (1998).
49. Wichterlová, B., and Cejka, J., *J. Catal.* **136**, 523 (1994).
50. Ivanova, I. I., Brunel, D., Nagy, J. B., Daelen, G., and Derouane, E. G., *Stud. Surf. Sci. Catal.* **78**, 587 (1993).
51. Ivanova, I. I., and Derouane, E. G., *Stud. Surf. Sci. Catal.* **85**, 361 (1994).
52. Ivanova, I. I., Brunel, D., Nagy, J. B., and Derouane, E. G., *J. Mol. Catal. A* **95**, 243 (1995).